# EVOLUTION OF A NOURISHED SAND BEACH

# UNDER LOW WAVE ENERGY IN THAILAND

# DURING 2015 - 2020

by

JIRAT LAKSANALAMAI AND NOBUHISA KOBAYASHI

RESEARCH REPORT NO. CACR-21-02
FEBRUARY 2021

CENTER FOR APPLIED COASTAL RESEARCH
University of Delaware
Newark, Delaware 19716

# ACKNOWLEDGMENTS

The first author is grateful to the support cordially received from various organizations in Thailand: Marine Department and Italian-Thai Development Public Co., Ltd. for providing the survey data as well as the information regarding the construction process; and Aquatic Resources Research Institute Chulalongkorn University (2012) and Aurora Technology and Engineering Consultant Co., Ltd. for sharing the useful resources regarding the design of beach nourishment at Pattaya beach. The first author was supported by the Office of the Civil Service Commission under the Government of Thailand, during his study at the Center for Applied Coastal Research, University of Delaware, Newark, Delaware.

## TABLE OF CONTENTS

## LIST OF TABLES

## LIST OF FIGURES

## ABSTRACT

Sand beaches are essential for coastal tourism in Thailand but erosion narrowed some beaches significantly. Pattaya is a famous resort near Bangkok in the upper Gulf of Thailand. The Pattaya beach is microtidal with the average tidal range of 1.5 m. The average significant wave height is 0.2 m and the wave energy is low. The beach was widened by placing 130 $m^3$/m of medium sand along the shoreline length of 2.8 km between two terminal groins constructed in 2018. The bathymetry and topography were measured in 2015, 2019, and 2020. Approximately 14% of the placed sand in the water depth less than 2 m was lost after one year as may be expected for nourished beaches under larger wave energy. The bathymetry changes in the water depth of 2-4 m varied alongshore. The sand volume change in this seaward zone of no wave breaking was as large as that in the landward sand placement zone. The assumption of negligible profile changes seaward of a closure depth is not applicable to this beach during 2015-2020.

# Chapter 1

# Introduction

Beach erosion is a chronic problem in Thailand. Coastal structures were built to reduce beach erosion but did not restore wide beaches expected for coastal resorts. Ritphring et al. (2018) compiled a database of beach characteristics, including sediment diameter and beach slope. 10% of Thailand's sandy coastlines are protected by seawalls and revetments. Most sediment diameters range between 0.2-0.5 mm. The average beach slope is 0.1. The average beach width above the mean sea level is 35 m. The first major beach nourishment in Thailand was carried out at Pattaya (Figure 1.1). This famous resort near Bangkok is located on the coast of the Gulf of Thailand which is about 400 km wide and 720 km long. The length of the upper (northern) square area is about 100 km and the average water depth is 15 m (Sojisuporn et al. 2013). In the following, the beach nourishment project is explained concisely. The bathymetry and topography data are analyzed to understand the evolution process of the nourished beach. The analyzed data are used to estimate the sand volume changes and sand transport patterns. The ultimate goal is to prolong the retention of the placed sand.

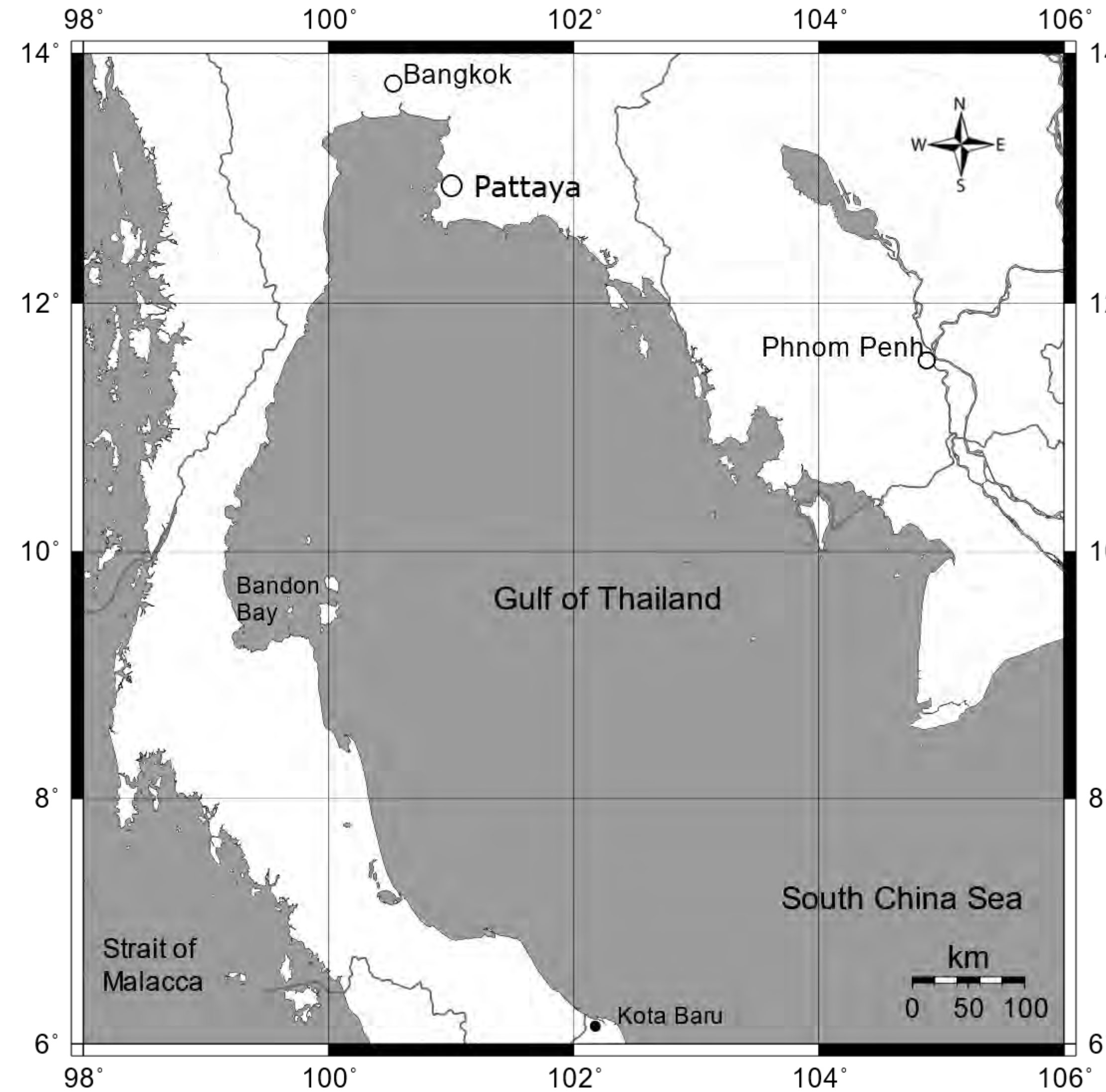


Figure 1.1 Pattaya beach location in Thailand (en.wikipedia.org/wiki/Gulf_of_Thailand).

# Chapter 2

## Pattaya Beach

Satellite images of Pattaya beach are available since 2005 (Google Earth Pro, TerraMetrics and Maxar Technologies). The dry beach width in the satellite images was very narrow even in 2005. This study deals with the interval of 2015-2020. Figure 2.1 shows satellite images from January 4, 2005 to November 25, 2019 well before and soon after the beach nourishment.

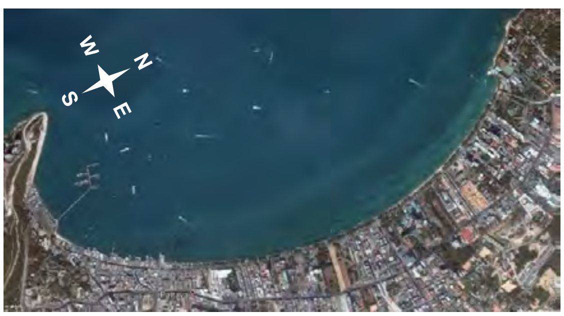


2005/01/04

2006/12/28

2007/12/31

2009/12/20

2013/01/31


2014/10/15

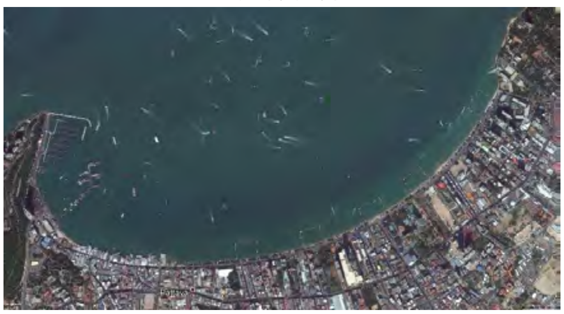
2015/03/01


2016/06/10


2016/09/08


2017/01/18


2018/02/12


2018/05/15


Figure 2.1 Pattaya beach (Google Earth Pro, TerraMetrics and Maxar Technologies) before and after beach nourishment.

The bathymetry and topography survey were conducted in December 2015, February 2019, and February 2020. The nourishment project was started in 2015 but it took time to locate an offshore borrow site with medium sand of 0.3-0.4 mm median diameter. The borrow site was at a distance of 20 km from Pattaya beach. Terminal groins were constructed in 2018. The sand was dredged and transported to a booster pump station ship. The transferred sand was pumped through pipelines on Pattaya beach along the curved shoreline of 2.8 km length between the terminal groins of 60 m length at the south and north (left and right in Figure 2.1) ends. The placed sand volume was 363,000 $m^3$, corresponding to the cross-sectional area increase of 130 $m^2$. The beach width above the mean sea level was 57 m. The foreshore slope was 0.1. Six photos in Figure 2.2 (a)-(f) show the transformation of Pattaya beach before, during and after the sand placement in 2018.

a. Pattaya beach (2015)

b. Pattaya beach (2015)

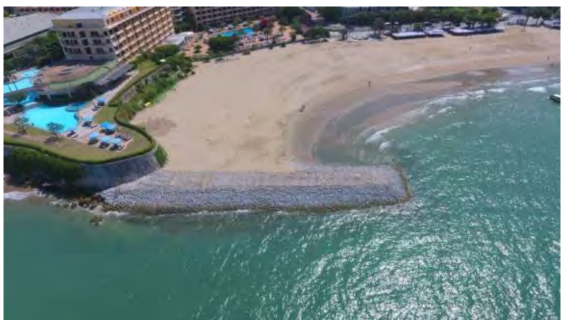

c. North terminal groin (2018)

d. South terminal groin (2018)

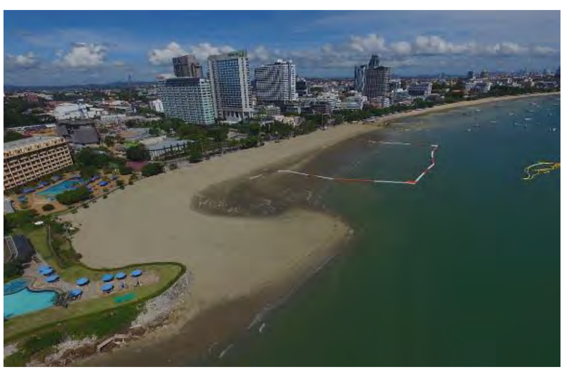

e. During sand placement (2018)

f. After sand placement (2019)

Figure 2.2 Pattaya beach before, during and after sand placement.

Continuous water level and wave data are not available in the vicinity of Pattaya. Intermittent tide gauge data at Ao Udom (Marine Department, 2018) located 20 km north of Pattaya were used to estimate water level variations relative to the mean sea level. The mean high and low water levels were 0.67 m and -0.83 m, respectively. The mean higher high-water level was 1.07 m and the highest high-water level including storm surge was 1.79 m. Storm surge is smaller in the Gulf of Thailand than in the Gulf of Mexico. Waves at Pattaya were estimated using the empirical formula in Coastal Engineering Manual (USACE 2003) and wind data at Pattaya Meteorological Station located 2.4 km south of Pattaya during 1981-2009. The formula was calibrated using wave buoy data during February-November, 1997. The average significant wave height and peak period were 0.2 m and 1.3 s, respectively. The maximum wave height and period were 2.1 m and 7.1 s, respectively. The predominant wave direction was from the south southwest.

Figure 2.3 shows the depth contours of 0-7 m at Pattaya beach in December 2015 before the nourishment and in February 2019 and 2020 after the nourishment where the north is rightward in this figure. The beach profiles were examined along 33 cross-shore lines (L1-L33) where six lines are shown for simplicity.

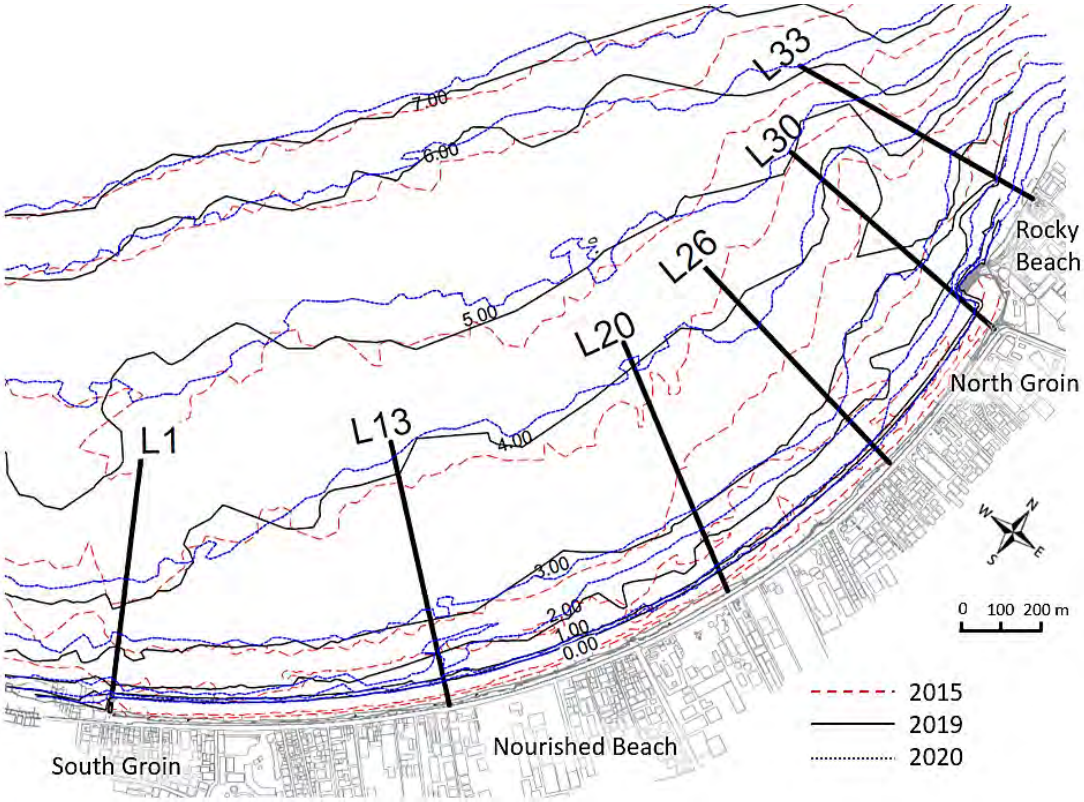


Figure 2.3 Depth contours in meters surveyed in December 2015, February 2019, and February 2020.

In Figure 2.3, L1 is immediately north of the south groin constructed to reduce local southward longshore sand transport observed at L1. Waves from the south are diffracted around the cape south of Pattaya (see Figure 2.1). The diffracted waves cause southward sand transport in the sheltered zone where a harbor was constructed. L30 is immediately south of the north groin constructed to reduce northward longshore sand transport. L33 is located on a rocky beach north of the nourished beach. The depth contours of 0-2 m between L1-L30 were affected by the sand placement before the 2019 survey. The depth contours of 2-4 m were relatively stationary between L1-L20 but migrated landward, resulting in erosion between L20-L30. L13 and L26 are located in the middle of L1-L20 and L20-L30, respectively.

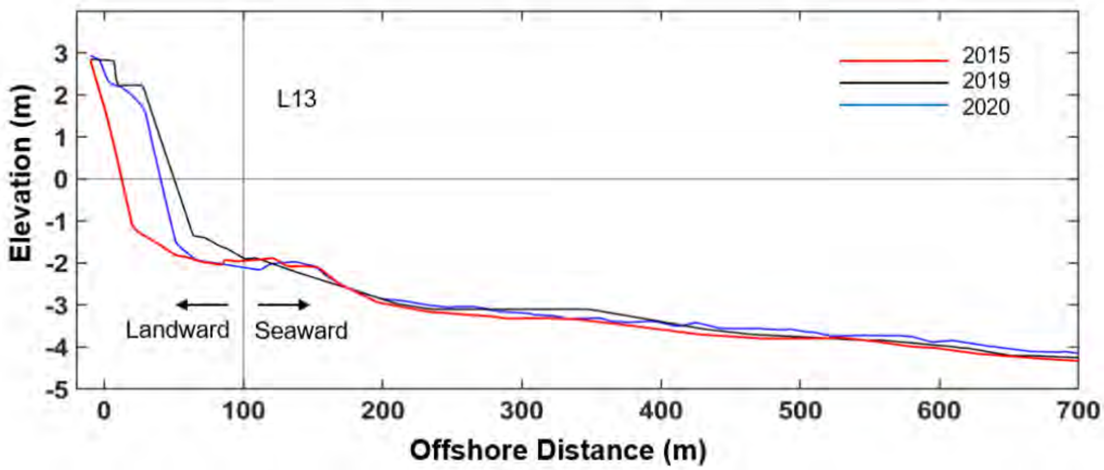


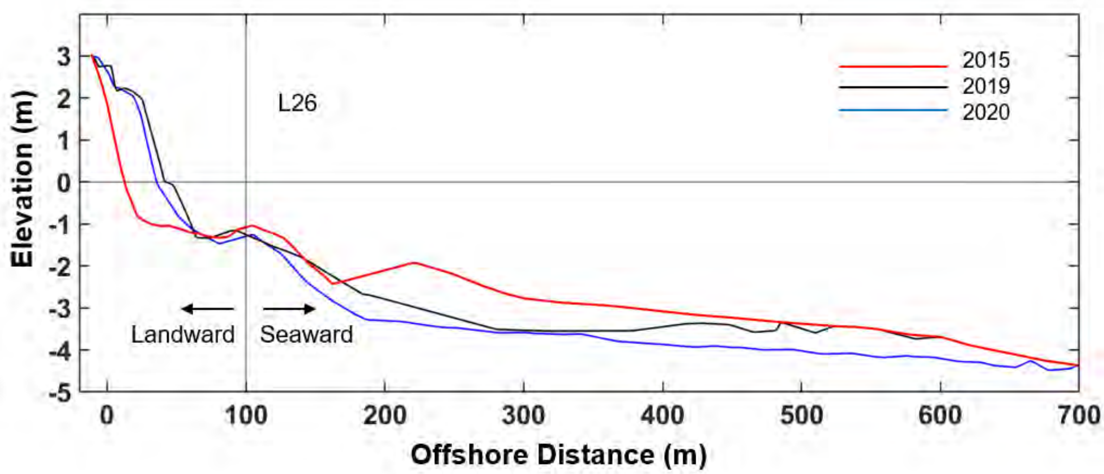


Figure 2.4 Beach profiles in 2015, 2019, and 2020 along Line L13 with offshore accretion and Line L26 with offshore erosion.

Figure 2.4 shows the beach profiles along L13 and L26 in 2015, 2019, and 2020. The elevation is relative to the mean sea level. The offshore distance is from the survey reference point located 10 m seaward of the vertical wall with its crest elevation of 3 m. The nourished berm elevation was increased from 2.2 m to 2.8 m in front of the wall. The beach profile evolution diverged at the offshore distance of approximately 100 m for L1-L30. The seaward limit was set at the offshore distance of 700 m of limited bottom elevation changes. The offshore distance of 100 m is used to separate the landward and seaward zones of different profile evolution patterns. The increase of the profile area in the landward zone from 2015 and 2019 may be regarded to represent the placed sand volume. The placed sand was eroded during 2019-2020. The water depth at this separation point decreased from about 2 m at L1 to 1 m at L30 because of the northward decrease of the beach slope in Figure 2.3. The seaward zone is accretional for L13 and erosional for L26. The bathymetric change for L26 was not expected for the microtidal beach of medium sand in the environment of low wave energy.

# Chapter 3

# Data Analysis

The beach profile data for L1-L30 are analyzed to explain the bathymetric changes during 2015-2020 in Figures 2.3 and 2.4. The bottom elevation $Z_b$ (x, t) relative to the mean sea level is presented as a function of the offshore distance x at given time t. The beach profile area change $\Delta A$ is calculated separately for the landward and seaward zones during December 2015 to February 2019 (3.2 years) and during February 2019 to February 2020 (1.0 year).

## 3.1 Beach profile area change

To interpret the beach profile area change $\Delta A$ for the 30 lines (L1 – L30), the area change $\Delta A$ is separated into;

$\Delta A_L$ = area change in the landward zone affected by beach nourishment

$\Delta A_S$ = area change in the seaward zone (not affected immediately)

As mentioned previously, the offshore distance of 100 m is used to separate the landward and seaward zones of different profile evolution patterns. Thus, the beach profile area change calculated separately for the landward and seaward zones are examined using x = 100 m as a separating point for the profiles $Z_b$ (x, t) with t = 2015, 2019, and 2020.

For landward zone;

$$\Delta A_L = \int_{-10\,m}^{100\,m} [Z_b(x,2020) - Z_b(x,2019)]dx \quad \text{for } 2019 - 2020$$

$$\Delta A_L = \int_{-10\,m}^{100\,m} [Z_b(x,2019) - Z_b(x,2015)]dx \quad \text{for } 2015 - 2019$$

For the seaward zone;

$$\Delta A_S = \int_{100\,m}^{700\,m} [Z_b(x,2020) - Z_b(x,2019)]dx \quad \text{for } 2019 - 2020$$

$$\Delta A_S = \int_{100\,m}^{700\,m} [Z_b(x,2019) - Z_b(x,2015)]dx \quad \text{for } 2015 - 2019$$

The total area change ΔA is given by $\Delta A = \Delta A_L + \Delta A_S$

In Table 3.1, the bottom elevation ($Z_b$) at x = 100 m and the beach profile area change $\Delta A_L$ and $\Delta A_S$ for L1 – L30 are summarized. The value of ($-Z_b$) is the water depth.

Table 3.1 Bottom elevation ($Z_b$) at x = 100 m and area changes $\Delta A_L$ and $\Delta A_S$ for L1 - L30

| **Line** | **$Z_b$ (m) at X = 100 m** | | | **area ($m^2$) changes (2015 - 2019)** | | **area ($m^2$) changes (2019 - 2020)** | |
|---|---|---|---|---|---|---|---|
| | **2015** | **2019** | **2020** | **$\Delta A_L$** | **$\Delta A_S$** | **$\Delta A_L$** | **$\Delta A_S$** |
| **L1** | -2.23 | -2.89 | -2.33 | -83.07 | -82.25 | 146.08 | 261.61 |
| **L2** | -2.07 | -2.10 | -2.35 | 211.27 | 31.62 | -26.22 | 30.79 |
| **L3** | -2.15 | -2.25 | -2.19 | 189.64 | 27.90 | -31.33 | -17.94 |
| **L4** | -2.12 | -1.95 | -2.22 | 176.85 | 22.01 | -30.52 | -19.21 |
| **L5** | -2.07 | -1.98 | -2.21 | 162.53 | -34.77 | -20.08 | -29.00 |
| **L6** | -2.06 | -1.75 | -2.25 | 175.51 | -12.46 | -45.65 | -57.07 |
| **L7** | -2.06 | -2.04 | -2.18 | 155.92 | -7.57 | -25.95 | -11.72 |
| **L8** | -2.07 | -1.97 | -2.14 | 153.49 | 0.99 | -41.17 | 34.33 |
| **L9** | -1.99 | -1.95 | -2.20 | 163.58 | 11.69 | -45.32 | 60.25 |
| **L10** | -2.00 | -2.08 | -2.04 | 162.02 | 27.24 | 40.02 | 64.95 |
| **L11** | -1.98 | -2.13 | -2.02 | 169.67 | 11.14 | -11.60 | 50.06 |
| **L12** | -1.98 | -2.08 | -1.89 | 159.06 | 14.89 | -9.10 | 57.90 |
| **L13** | -1.95 | -1.88 | -2.10 | 164.80 | 48.85 | -57.41 | 26.14 |
| **L14** | -1.94 | -1.82 | -2.19 | 161.20 | 105.14 | 8.35 | 6.32 |
| **L15** | -1.89 | -1.77 | -1.99 | 158.53 | 67.48 | -49.99 | 41.22 |
| **L16** | -1.96 | -1.87 | -1.98 | 147.65 | 65.19 | -60.02 | 57.13 |
| **L17** | -1.82 | -1.84 | -1.95 | 143.59 | 102.85 | -44.14 | 16.40 |
| **L18** | -2.28 | -1.83 | -1.81 | 168.40 | 81.82 | 24.53 | 79.06 |
| **L19** | -2.07 | -1.95 | -1.63 | 122.27 | 2.47 | 35.09 | 94.73 |
| **L20** | -1.88 | -2.02 | -1.75 | 113.35 | -2.12 | 12.64 | -6.10 |
| **L21** | -1.63 | -1.61 | -1.87 | 102.55 | -28.94 | -20.83 | -62.88 |
| **L22** | -1.33 | -1.29 | -1.53 | 86.20 | 8.78 | -40.75 | -174.01 |
| **L23** | -1.74 | -1.50 | -1.46 | 77.56 | -73.98 | -15.24 | -135.90 |
| **L24** | -1.36 | -1.41 | -1.28 | 86.19 | -122.58 | -10.60 | -121.97 |
| **L25** | -1.09 | -1.44 | -1.22 | 82.27 | -133.59 | 15.04 | -187.79 |
| **L26** | -1.08 | -1.25 | -1.30 | 103.18 | -200.35 | -23.55 | -214.94 |
| **L27** | -1.05 | -1.31 | -1.15 | 102.15 | -213.61 | -25.28 | -207.70 |
| **L28** | -1.10 | -1.19 | -1.13 | 112.44 | -197.32 | -29.17 | -201.07 |
| **L29** | -1.19 | -1.20 | -1.19 | 127.29 | -349.90 | -31.05 | -68.50 |
| **L30** | -1.15 | -0.99 | -1.08 | 191.05 | -371.53 | -35.60 | -77.60 |

### 3.2 Alongshore length along Pattaya beach

The alongshore distance from L1 is calculated for each of the 30 cross-shore lines whose alongshore spacing decreases offshore. The area between L1-L30 is separated into 29 segments in the landward and seaward zones. The alongshore segment length in the landward (seaward) zone is calculated as the segment area divided by the cross-shore distance of 110 m (600 m) in the landward (seaward) zone. The alongshore distance from L1 is the cumulative segment length from the first segment between L1 and L2. The alongshore distance from L1 to L30 is 2660 m and 2280 m in the landward and seaward zones, respectively. The calculation procedure is explained in detail in the following.

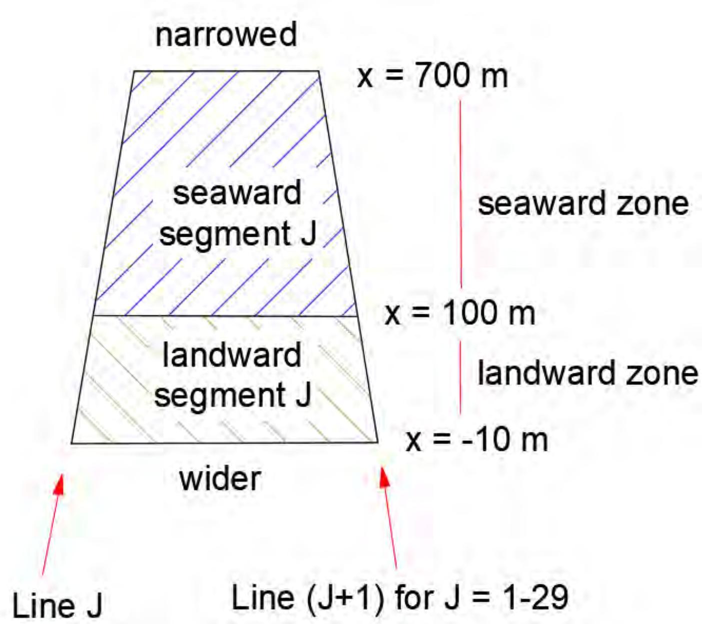


Figure 3.1 Horizontal areas between cross-shore lines and along x = 100 m separating landward and seaward zones.

The alongshore length and segment area are calculated using Figure 3.1. Segment J represents the area between Line J and (J+1) from x = (-10)-700 m. The beach has a curved alignment and the cross-shore lines are not parallel. The alongshore distance decreases seaward. The horizontal area in the seaward (landward) segment is divided by the cross-shore length of the seaward (landward) segment to obtain alongshore length which is the average alongshore length based on the segment horizontal area. The cross-shore length, horizontal area, and alongshore length of 29 segments are listed in Table 3.2.

Table 3.2 "Landward" and "Seaward" horizontal area and alongshore length for segments S1-S29

| Segment | Cross-shore length (m) | | Horizontal area ($m^2$) | | Alongshore length (m) | |
|---|---|---|---|---|---|---|
| | **landward** | **seaward** | **landward** | **seaward** | **landward** | **seaward** |
| **S1** | 110 | 600 | 10,784 | 48,133 | 98.04 | 80.22 |
| **S2** | 110 | 600 | 5,551 | 32,621 | 50.46 | 54.36 |
| **S3** | 110 | 600 | 5,155 | 12,904 | 46.86 | 21.50 |
| **S4** | 110 | 600 | 5,596 | 34,889 | 50.87 | 58.14 |
| **S5** | 110 | 600 | 11,065 | 63,131 | 100.59 | 105.21 |
| **S6** | 110 | 600 | 10,808 | 50,570 | 98.25 | 84.28 |
| **S7** | 110 | 600 | 5,194 | 15,204 | 47.22 | 25.34 |
| **S8** | 110 | 600 | 5,508 | 30,561 | 50.08 | 50.93 |
| **S9** | 110 | 600 | 10,847 | 52,120 | 98.61 | 86.86 |
| **S10** | 110 | 600 | 5,524 | 31,181 | 50.22 | 51.96 |
| **S11** | 110 | 600 | 5,414 | 25,838 | 49.22 | 43.06 |
| **S12** | 110 | 600 | 15,873 | 59,386 | 144.30 | 98.97 |
| **S13** | 110 | 600 | 10,682 | 44,577 | 97.11 | 74.29 |
| **S14** | 110 | 600 | 10,977 | 58,768 | 99.79 | 97.94 |
| **S15** | 110 | 600 | 10,713 | 46,077 | 97.39 | 76.79 |
| **S16** | 110 | 600 | 16,521 | 88,529 | 150.20 | 147.54 |
| **S17** | 110 | 600 | 15,980 | 61,171 | 145.27 | 101.95 |
| **S18** | 110 | 600 | 16,381 | 81,636 | 148.92 | 136.06 |
| **S19** | 110 | 600 | 5,961 | 52,154 | 54.19 | 86.92 |
| **S20** | 110 | 600 | 5,494 | 29,582 | 49.94 | 49.30 |
| **S21** | 110 | 600 | 16,073 | 67,757 | 146.12 | 112.93 |
| **S22** | 110 | 600 | 10,909 | 49,641 | 99.17 | 82.73 |
| **S23** | 110 | 600 | 10,273 | 25,378 | 93.39 | 42.29 |
| **S24** | 110 | 600 | 10,644 | 42,017 | 96.77 | 70.02 |
| **S25** | 110 | 600 | 5,340 | 22,014 | 48.54 | 36.69 |
| **S26** | 110 | 600 | 10,694 | 45,203 | 97.22 | 75.33 |
| **S27** | 110 | 600 | 5,470 | 28,613 | 49.73 | 47.68 |
| **S28** | 110 | 600 | 16,442 | 86,810 | 149.48 | 144.68 |
| **S29** | 110 | 600 | 16,404 | 83,862 | 149.13 | 139.77 |
| | **Sum** | | **292,292** | **1,370,340** | **2,657.20** | **2,283.90** |

### 3.3 Alongshore variation of erosion and accretion

Cross-sectional area change (ΔA) (sand volume change per unit alongshore length) at Line J (J=1-30) is used to examine the alongshore variation of sand loss or gain per unit length ($m^3/m$). (ΔA) is plotted as a function of the alongshore distance of Line J which is the sum of "landward" segment alongshore length for Segments 1 to (J-1). The following symbols are used for plotting.

| | 2015-2019 | 2019-2020 |
|---|---|---|
| Landward | ○ | △ |
| Seaward | ● (blue) | ▲ (blue) |

The four different values of ΔA in the two zones and during the two intervals are plotted for each of the 30 cross-shore lines in Figure 3.2 as a function of the landward alongshore distance from L1.

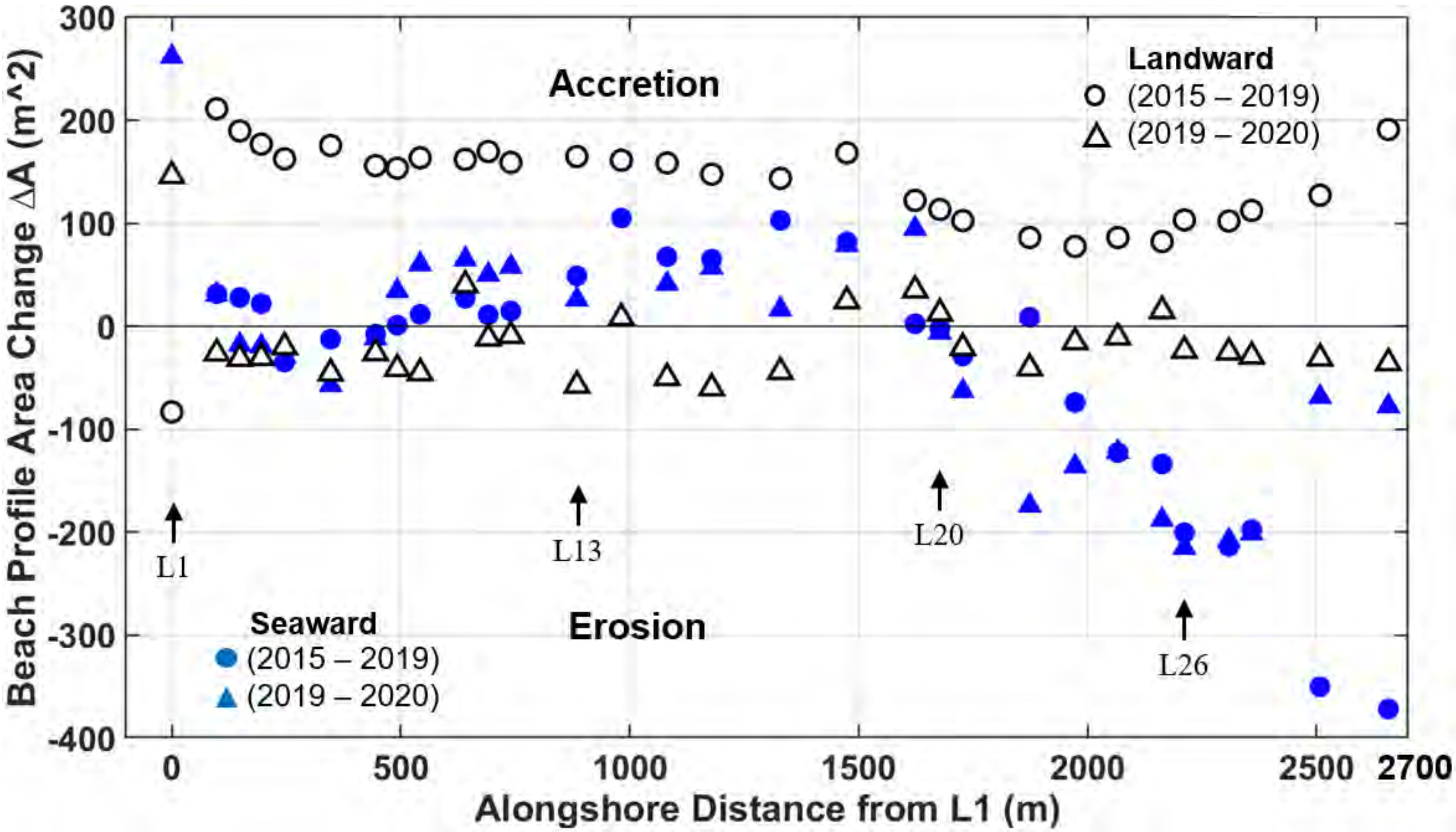


Figure 3.2 Beach profile area change ΔA in landward and seaward zones along L1–L30 during 2015–2019 and 2019–2020.

The area change ΔA in the landward zone during 2015-2019 was positive (accretion) for L2-L30 because of the sand placement before the 2019 survey. No sand was placed along L1 because sand accretion was expected north of the south groin. The erosional area change ΔA was almost the same in the landward and seaward zones of L1 during 2015-2019 (see Table 3.1). The area change ΔA in the landward zone during 2019-2020 was negative (erosion) except for L1, 10, 14, 18-20, and 25 where sand accretion occurred. Sand was deposited north of the south groin in the landward and seaward zones of L1 during 2019-2020. The area changes in the seaward zone during 2015-2019 and 2019-2020 were mostly positive for L2-L20 and negative for L21-L30. The effect of the beach nourishment was not apparent in the seaward zone. L1 is excluded from the following data analysis.

### 3.4 Correlation among different area changes

The area change ΔA in the landward zone during 2019-2020 indicates loss of the placed sand. Figure 3.3 compares the area changes in the landward zone along the same cross-shore line during 2015-2019 (sand placement) and during 2019-2020 (sand loss). The slight negative correlation among the scattered data points implies the increase of sand loss with the increase of the placed sand volume. The negative slope of 0.14 suggests that about 14% of the placed sand was lost after one year.

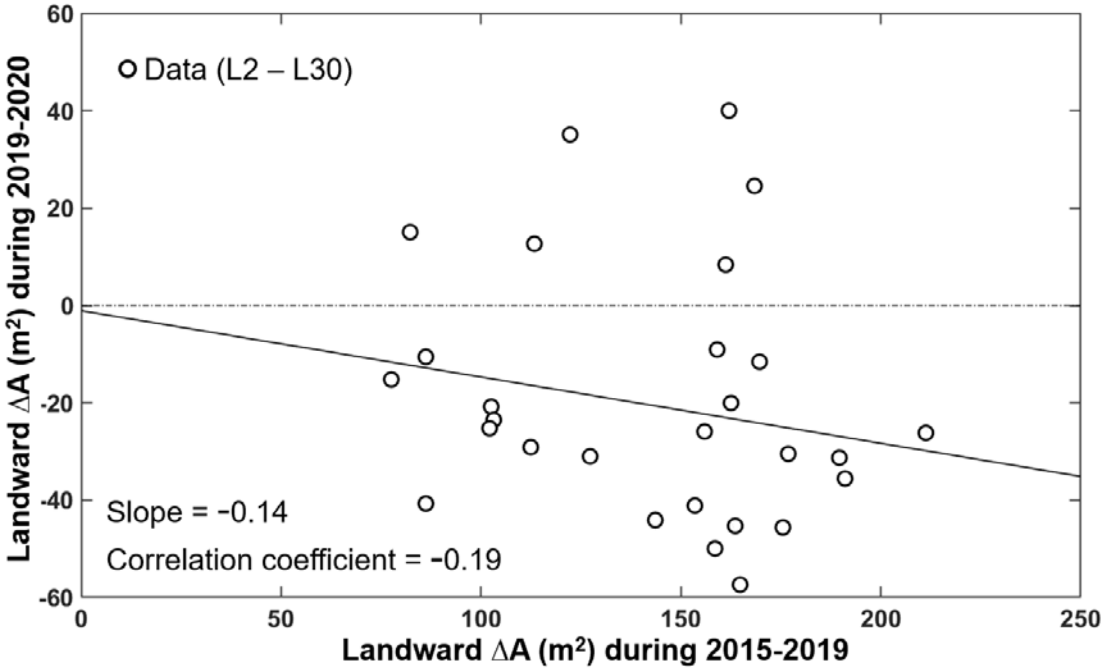


Figure 3.3 Correlation between landward ΔA (including nourished sand) during 2015–2019 and landward ΔA (loss of nourished sand) during 2019–2020.

Sand placed on the foreshore of a sand beach is transported in the cross-shore and longshore directions. Figlus and Kobayashi (2008) analyzed the profile area changes of four nourished beaches in Delaware during 1998-2005. The average significant wave height and peak period were 1.3 m and 7.5 s during 1998-2005. The transition between the landward and seaward zones was in the water depth of 1.3-1.9 m corresponding to the breaker zone of average waves. The area changes in the landward and seaward zones were correlated with the negative correlation coefficient of -0.67 to -0.85. Erosion in the landward (seaward) zone resulted in accretion in the seaward (landward) zone due to offshore (onshore) sand transport. Figure 3.4 compares the area changes in the seaward and landward zones during 2019-2020. The scattered data points with the correlation coefficient of 0.12 and the slope of 0.03 suggest little correlation between the two zones. The offshore distance of 100 m used to separate the landward and seaward zones (see Figure 2.4) is located seaward of the breaker zone of average waves of 0.2 m height at Pattaya beach. The bathymetric changes in the seaward zone cannot be explained by breaking waves and wave-induced currents.

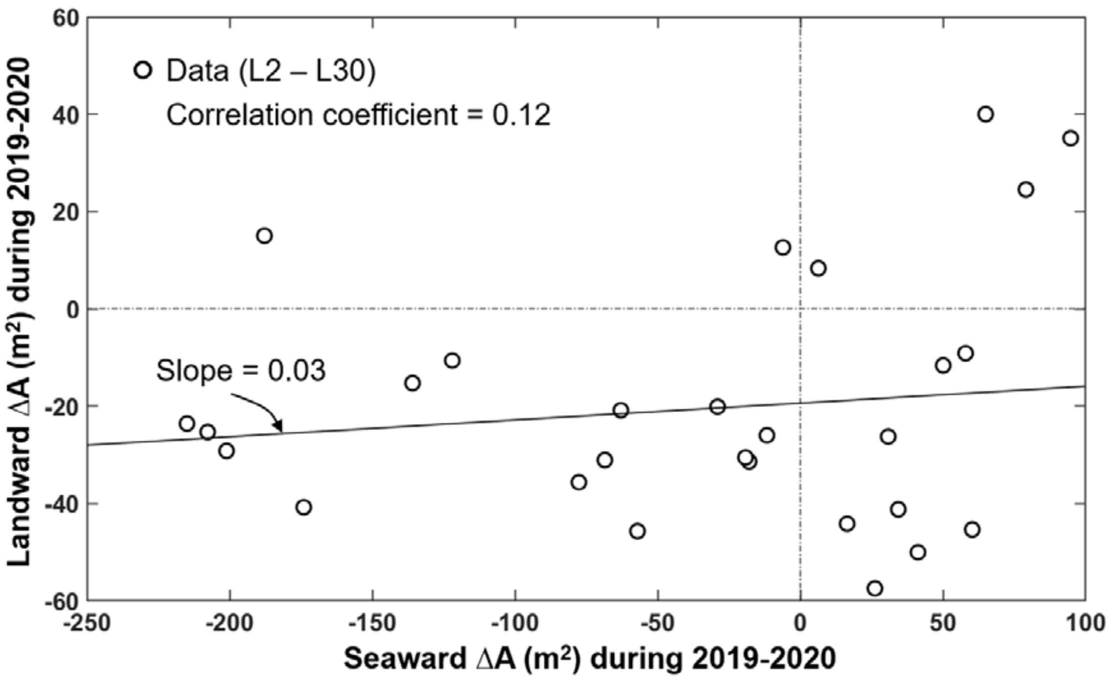


Figure 3.4 Correlation between seaward ΔA and landward ΔA during 2019–2020 where the correlation should be negative if the nourished sand is transported offshore and deposited in the seaward zone.

Figure 3.5 compares the area changes in the seaward zone during 2015-2019 (3.2 years) and 2019-2020 (1.0 year). The correlation coefficient of 0.66 with the slope of 0.85 indicates the continuous bathymetric change in the seaward zone before and after the beach nourishment. The rate of the change increased in view of the interval difference between 1.0 and 3.2 years. The bathymetric change in the seaward zone might have been caused by tidal currents. Offshore tidal currents were measured in 1993. Flood and ebb tidal currents were in the range of 0.3-0.5 m/s. The numerical prediction of sand transport by waves and currents is beyond the scope of this study.

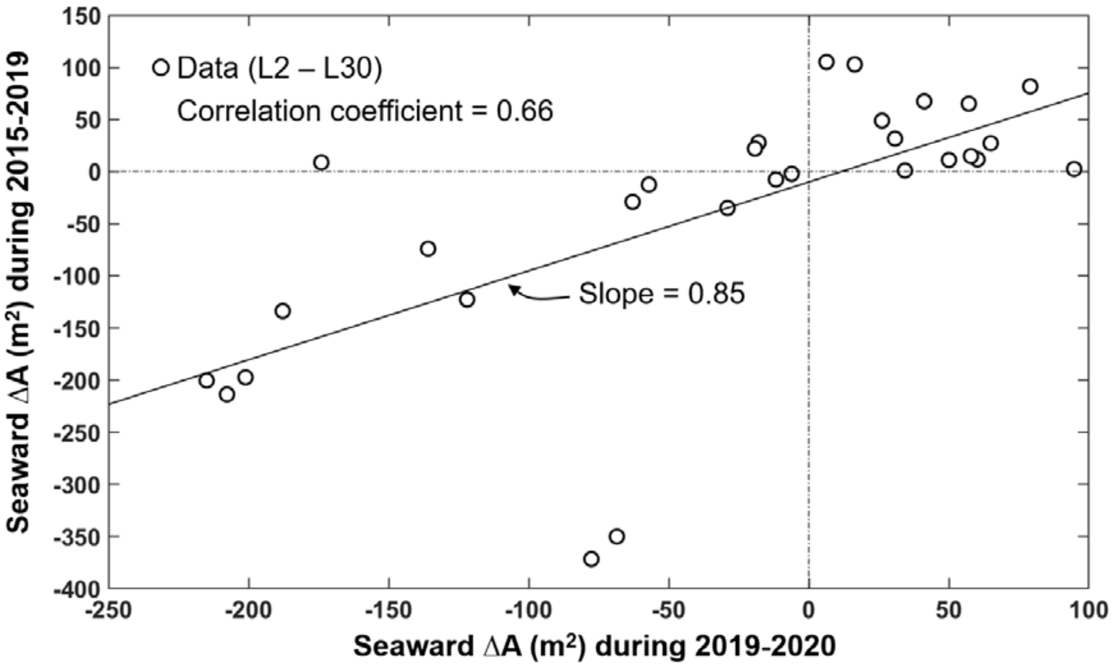


Figure 3.5 Correlation between seaward ΔA during 2019–2020 and seaward ΔA during 2015–2019 where the positive correlation implies the continuation of the bathymetric change in the seaward zone before and after the beach nourishment.

### 3.5 Sand volume changes

Sand volume changes in the landward and seaward zones between L1-L20 and L20-L30 are calculated (Table 3.3) and presented in Figure 3.6. All the cross-shore lines are represented by three points at the offshore distance of -10, 100, and 700 m. The curved line of -10 m corresponds to the vertical wall with its crest elevation of 3 m. The curved line of 100 m separating the landward and seaward zones terminates near the head of the north groin. The curved line of 700 m is the seaward boundary of noticeable bottom elevation changes in this study but the bottom elevation changed somewhat outside the study area (Figure 2.3).

Sand volume change ($\Delta V$) in Table 3.3 is calculated using the alongshore length of each segment (Table 3.2) and the beach profile area change along each cross-shore line (Table 3.1) as follows:

Sand volume change ($\Delta V$) for landward (seaward) Segment J = alongshore length of landward (seaward) Segment J x average of the profile area changes along Lines J and (J+1) where the definitions of segment J and Line J are shown in Figure 3.1. The sand volume changes in each of the four areas during 2015-2019 and 2019-2020 are shown in Table 3.3, where the nourished sand volume is included in the landward zone for 2015-2019.

Table 3.3 Sand volume change ΔV ($m^3$) in landward and seaward zones during 2015-2019 and 2019-2020

| **Segment** | **Volume change ΔV ($m^3$)** | | | |
|---|---|---|---|---|
| | **2015-2019** | | **2019-2020** | |
| | **landward** | **seaward** | **landward** | **seaward** |
| S1 | 6,285 | -2,030 | 5,875 | 11,728 |
| S2 | 10,115 | 1,618 | -1,452 | 349 |
| S3 | 8,588 | 536 | -1,449 | -399 |
| S4 | 8,633 | -370 | -1,287 | -1,401 |
| S5 | 17,002 | -2,484 | -3,305 | -4,528 |
| S6 | 16,282 | -844 | -3,517 | -2,898 |
| S7 | 7,306 | -83 | -1,584 | 286 |
| S8 | 7,939 | 322 | -2,165 | 2,408 |
| S9 | 16,053 | 1,690 | -261 | 5,437 |
| S10 | 8,329 | 997 | 713 | 2,988 |
| S11 | 8,090 | 560 | -509 | 2,324 |
| S12 | 23,367 | 3,154 | -4,798 | 4,159 |
| S13 | 15,829 | 5,720 | -2,382 | 1,205 |
| S14 | 15,953 | 8,453 | -2,077 | 2,328 |
| S15 | 14,910 | 5,094 | -5,357 | 3,776 |
| S16 | 21,872 | 12,397 | -7,822 | 5,424 |
| S17 | 22,662 | 9,413 | -1,424 | 4,866 |
| S18 | 21,643 | 5,734 | 4,439 | 11,822 |
| S19 | 6,384 | 15 | 1,293 | 3,852 |
| **S1-S19** | **257,249** | **49,895** | **-27,074** | **53,731** |
| S20 | 5,391 | -765 | -204 | -1,700 |
| S21 | 13,790 | -1,138 | -4,499 | -13,375 |
| S22 | 8,120 | -2,697 | -2,776 | -12,820 |
| S23 | 7,646 | -4,157 | -1,206 | -5,453 |
| S24 | 8,151 | -8,969 | 214 | -10,846 |
| S25 | 4,501 | -6,126 | -206 | -7,388 |
| S26 | 9,981 | -15,593 | -2,373 | -15,920 |
| S27 | 5,335 | -9,798 | -1,353 | -9,746 |
| S28 | 17,917 | -39,587 | -4,500 | -19,501 |
| S29 | 23,737 | -50,417 | -4,969 | -10,210 |
| **S20-S29** | **104,575** | **-139,250** | **-21,876** | **-106,963** |
| **Total** | **361,825** | **-89,355** | **-48,951** | **-53,232** |

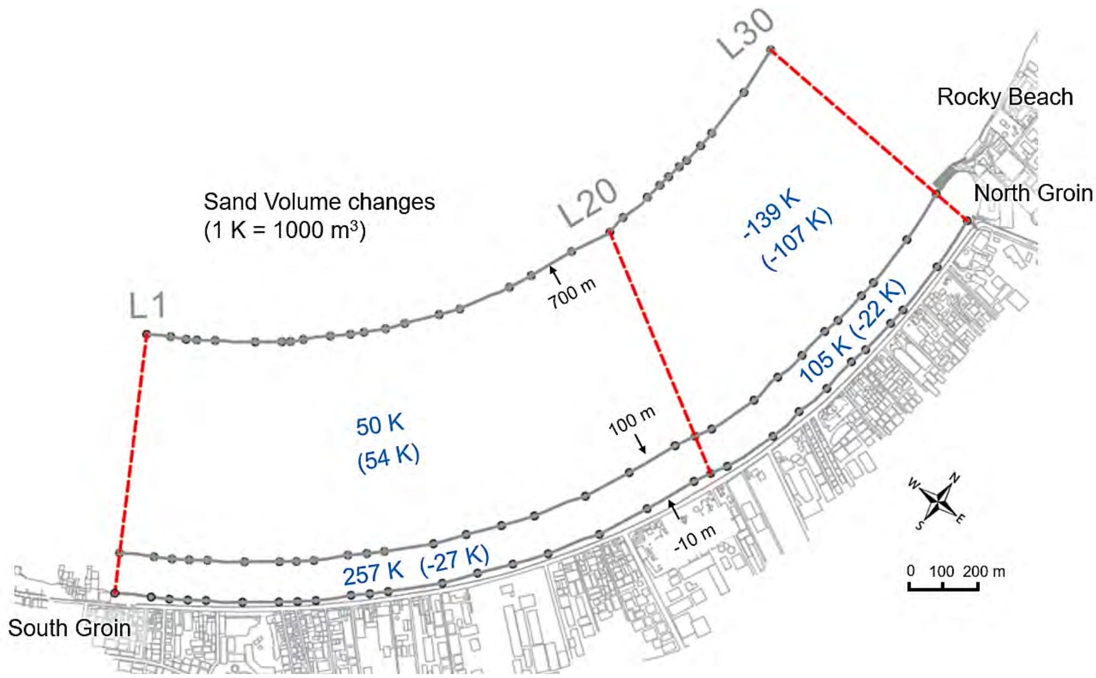


Figure 3.6 Sand volume changes in the landward and seaward zones during 2015–2019 in comparison with those (in parentheses) during 2019–2020 where points (solid circles) along each of L1–L30 are located at the offshore distances of -10, 100 and 700 m.

Figure 3.6 presents the measured sand volume changes concisely. The sand placement in the landward zone before the 2019 survey increased the sand volume by 257K (1K=1,000 $m^3$) and 105K between L1-L20 and L20-L30, respectively. The sum of 362K is practically the same as the nourished sand volume of 363K. This confirms the sand placement between L1 and L30. The negative values in the parentheses indicate the lost sand volumes during 2019-2020. The total lost volume was 49K and 13.5% of 362K. This sand loss rate is consistent with the statistical result in Figure 3.3. The destination of the lost sand was searched in the survey data. The lost sand could have been transported northward by waves from the southwest and deposited behind the north groin and north of L30. However, the sand volume change in this area was -7K during 2019-2020. This area was essentially full because of the sand placement in 2018 (Figures 2.1 and 2.2). The sum of 49K and 7K is the volume of the lost sand from the landward zone including the area behind the north groin. The lost sand volume of 56K must have been transported offshore to the seaward zone during 2019-2020.

In the seaward zone, the deposited sand volume between L1-L20 was 50K (54K) during 2015-2019 (2019-2020) and the eroded sand volume between L20-L30 was 139K (107K) during 2015-2019 (2019-2020). The deposited sand volume of 54K between L1-L20 during 2019-2020 was similar to the lost sand volume of 56K from the landward zone but there was little correlation between the profile area changes in the two zones (Figure 3.4). The profile area changes in the seaward zone during 2015-2019 and 2019-2020 were correlated (Figure 3.5) but the accretion and erosion processes in the seaward zone are uncertain. The lost sand of 56K during 2019-2020 could have been transported to the seaward zone between L20-L30 and farther northward. The bathymetric changes on the rocky beach north of L30 and the beach profile changes along L31-L33 (see Figure 2.3) were examined to locate the destination of eroded sand in the seaward zone between L20-L30. Sand volume of 94K was deposited north of L30 in the seaward zone of L31-L33 during 2019-2020. This finding may support the conjecture of northward sand transport and deposition during 2019-2020 but the same area was eroded more during 2015-2019. Consequently, the eroded sand destination is still uncertain.

# Chapter 4

## Conclusions

The first major beach nourishment project under low wave energy in Thailand was assessed using the bathymetry and topography survey data before and after the nourishment. The nourished berm with the foreshore slope of 0.1 was eroded like a nourished beach under high or medium wave energy but no bar was formed seaward of the eroded zone. No sand accretion was found behind a terminal groin. Morphological changes associated with breaking waves and wave-induced currents were subdued or absent. The destination of sand eroded from the foreshore was uncertain. In the seaward zone outside the surf zone, bathymetric changes during 2019-2020 were affected little by the foreshore erosion. Measurements of currents, waves, and sand transport are required to clarify the causes of the bathymetric changes in the seaward zone. Sand transfer between the landward and seaward zones may become more apparent after several years. The bathymetry and topography survey should be continued to improve the design of beach nourishment in the environment of low wave energy and limited availability of sand.

## REFERENCES

Figlus, J., and Kobayashi, N., 2008. "Inverse estimation of sand transport rates on nourished Delaware beaches". J. Waterway, Port, Coastal and Ocean Eng., 134(4), 218-225.

Ritphring, S., Somphong, C., Udo, K., and Kazama, S., 2018. "Projections of future beach loss due to sea level rise for sandy beaches along Thailand's coastlines." J. Coastal Research, 85(sp1), 541-545.

Sojisuporn, P., Sangmanee, C., and Wattayakorn, G., 2013. "Recent estimate of sea-level rise in the Gulf of Thailand." Maejo Int. J. Sci. Technol., 7(Special Issue), 106-113.

USACE (United States Army Corps of Engineers), 2003. "Coastal Engineering Manual. Washington, DC: USACE